

How Important is the Back Reaction of Electrons via the Substrate in Dye-Sensitized Nanocrystalline Solar Cells?

Petra J. Cameron and Laurence M. Peter*

Department of Chemistry, University of Bath, BA2 7AY, United Kingdom

Sarmimala Hore

Freiburg Materials Research Center, Stefan-Meier Strasse 21, D-79110 Freiburg, Germany

Received: August 23, 2004; In Final Form: October 25, 2004

The role of the conducting glass substrate (fluorine-doped tin oxide, FTO) in the back reaction of electrons with tri-iodide ions in dye-sensitized nanocrystalline solar cells (DSCs) has been investigated using thin-layer electrochemical cells that are analogues of the DSCs. The rate of back reaction is dependent on the type of FTO and the thermal treatment. The results show that this back-reaction route cannot be neglected in DSCs, particularly at lower light intensities, where it is the dominant route for the back transfer of electrons to tri-iodide. This conclusion is confirmed by measurements of the intensity dependence of the photovoltages of DSCs with and without blocking layers. It follows that blocking layers should be used to prevent the back reaction in mechanistic studies in which the light intensity is varied over a wide range. Conclusions based on studies of the intensity dependence of the parameters of DSCs such as photovoltage and electron lifetime in cells without blocking layers, must be critically re-examined.

Introduction

The active absorber layer in the original dye-sensitized nanocrystalline cell (DSC) that was developed by O'Regan and Grätzel¹ consists of a thin (typically 10 μm) dye-coated layer of sintered nanocrystalline anatase on a transparent conducting glass (fluorine-doped tin oxide, FTO). The redox electrolyte is the tri-iodide/iodide (I_3^-/I^-) couple in an organic solvent such as acetonitrile, and the counter electrode in the sandwich cell is platinum-coated FTO. One of the interesting features of the DSC is that the collection of photoinjected electrons by diffusion through the TiO_2 matrix is very efficient under short-circuit conditions: incident photon to current conversion efficiencies (IPCEs) as high as 90% are routinely reported.² This indicates that the back reaction of photoinjected electrons with I_3^- is relatively unimportant at short circuit, so that the diffusion length of electrons exceeds the film thickness.^{3–6} By contrast, catalyzed regeneration of I^- from I_3^- at the platinized counter electrode is fast, and voltage losses at the counter electrode are generally small.⁷ More-recent variants of the DSC have utilized alternative "hole transport media", including cobalt redox complexes^{8–10} or solid-state organic hole conductors.^{11–13} By contrast with the original (I_3^-/I^-)-based cell, these cells only function satisfactorily if a thin blocking underlayer of TiO_2 is deposited on the FTO via spray pyrolysis, to prevent "shunting" by electron transfer from the FTO substrate.

We have recently characterized the kinetics of electron transfer for the I_3^-/I^- (see ref 7) and $[\text{Co}(\text{dbbip})_2]^{3+/2+}$ (dbbip = 2,6-bis(1'-butylbenzimidazol-2'-yl)pyridine)¹⁴ redox couples at bare and blocked FTO electrodes, using thin-layer cells that mimic the operation of the DSC. The results show that the rate of electron exchange between both redox couples and the

substrate is dependent on whether a blocking layer is present. The thin continuous blocking layers of TiO_2 , which are produced by spray pyrolysis, are typically <100 nm thick. They are moderately *n*-doped and display rectification characteristics, blocking oxidation of the reduced component of the redox couples but allowing some reduction of the oxidized component as the band bending is reduced and electrons accumulate at the interface. Uncoated FTO layers, on the other hand, do not display rectifying characteristics, and significant losses by back-electron transfer may be expected for DSCs operating under load conditions, even in the case of the I_3^-/I^- redox couple. In the present study, we attempt to establish how significant these losses are under different conditions and how back reaction at the FTO influences measured characteristics such as the intensity dependence of the photovoltage. Thin-layer cells were constructed with and without TiO_2 blocking layers and with and without nanocrystalline TiO_2 layers. The current–voltage behavior of these cells has provided new insights into the influence of surface preparation, thermal treatment, and blocking layers on the importance of back reaction via the substrate.

The results of theoretical calculations performed using different values of the exchange current density (j_0) for the redox shuttle show that back reaction via the substrate should become more important at lower light intensities. This prediction has been confirmed by measurements of the intensity dependence of the photovoltage for DSCs with and without blocking layers. The implications of the present work for the interpretation of dynamic measurements—photovoltage decay,¹⁵ charge extraction,^{16,17} and intensity-modulated photovoltage spectroscopy (IMVS)^{18,19}—are considered elsewhere.¹⁵

Theory

Figure 1 illustrates the three routes that must be considered for the back reaction of electrons with the oxidized partner of

* Author to whom correspondence should be addressed. Telephone: +44 1225 386815. Fax: +44 1225 385802. E-mail address: l.m.peter@bath.ac.uk.

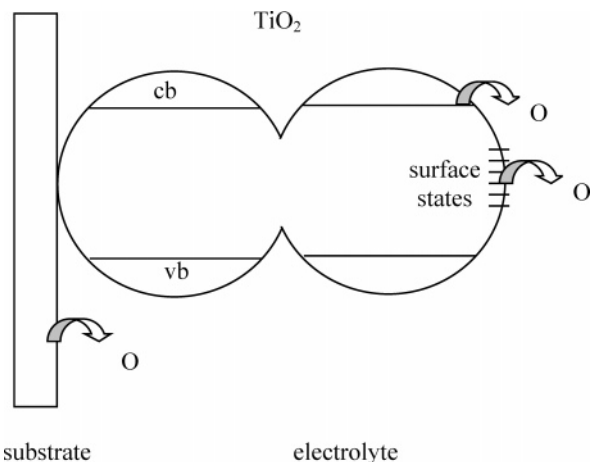


Figure 1. Schematic illustration of the three routes for the back reaction of photoinjected electrons with the oxidized component of the redox electrolyte in a dye-sensitized nanocrystalline solar cell (DSC).

the redox system in the DSC. The first two routes involve transfer of electrons from the nanocrystalline TiO_2 , either via the conduction band or via surface states, respectively. In the case of the third route, electrons are transferred from the highly conducting FTO substrate to redox species in the electrolyte. Under photostationary conditions (zero net current flow in the external circuit of the DSC), the rate of electron injection from the photoexcited dye is balanced by the sum of the rates of all three back-reaction pathways, provided that electron transfer to the oxidized dye can be neglected.

Electron Transfer from the Conduction Band of the Nanocrystalline TiO_2 . In the Boltzmann limit of the Fermi Dirac distribution, the photostationary density of electrons in the conduction band of the TiO_2 particles is given by

$$n_{\text{cb}} = N_{\text{cb}} \exp\left(-\frac{E_{\text{cb}} - {}_nE_{\text{F}}}{k_{\text{B}}T}\right) \quad (1)$$

where ${}_nE_{\text{F}}$ is the quasi Fermi level for electrons and the other symbols have their usual meanings. In darkness, the density of conduction band electrons is given by

$$n_{\text{cb,dark}} = N_{\text{cb}} \exp\left(-\frac{E_{\text{cb}} - E_{\text{F,redox}}}{k_{\text{B}}T}\right) \quad (2)$$

where $E_{\text{F,redox}}$ is the redox Fermi level. Equation 1 can therefore be rewritten in terms of the photovoltage, U_{photo} , as

$$n_{\text{cb}} = n_{\text{cb,dark}} \exp\left(\frac{qU_{\text{photo}}}{k_{\text{B}}T}\right) \quad (3)$$

where qU_{photo} corresponds to the difference between the Fermi levels in the TiO_2 in darkness and under illumination.

Under the conditions of interest, we may assume that $n_{\text{cb}} \gg n_{\text{cb,dark}}$, and the rate of first-order back reaction of electrons in the nanocrystalline TiO_2 with the redox species O, in the absence of substantial variations in the concentration of O, is therefore

$$v_{\text{cb}} = k'_{\text{cb}} n_{\text{cb}} [\text{O}] = k_{\text{cb}} n_{\text{cb}} \quad (4)$$

where k_{cb} is a pseudo first-order rate constant ($k_{\text{cb}} = k'_{\text{cb}} [\text{O}]$, given in units of s^{-1}). A more-general expression can be formulated for the case where the rate is higher order in electron concentration, but the experimental results presented in the present paper suggest that the rate-determining step in the reduction of I_3^- is first order in electron concentration. Note

here that our previous conclusion⁶ — that the reaction is second order in electron concentration — is questionable, because it was based on the measurements of the intensity dependence of the IMVS relaxation constant for cells without a blocking layer.

For a film of thickness d , the rate of the back reaction via the conduction band corresponds to a current density that is given by

$$j_{\text{cb}} = -qdk_{\text{cb}}n_{\text{cb}} \quad (5)$$

(We follow the convention that electron transfer to O corresponds to a negative current.)

Electron Transfer via Surface States. Nanocrystalline TiO_2 clearly contains a high density of electron traps that slow electron transport. A pertinent question is whether these trapping states are restricted to the bulk or to the surface, or whether both bulk and surface states are present. As far as electron transfer to redox species is concerned, it is the surface states that are important. In the case of a distribution of surface state energies, this is a more-complex problem than reaction via the conduction band, because the Marcus model predicts that the rate constant for electron transfer should be dependent on the reorganization energy of the redox system and on the standard free-energy difference.²⁰ Here, we use a simplified approach to obtain qualitative insight while maintaining simplicity. We use a global first-order rate constant k_{ss} to describe electron transfer to oxidized species via surface states and express the corresponding current density by analogy with eqs 4 and 5 as

$$j_{\text{ss}} = -qdk_{\text{ss}}n_{\text{ss}} \quad (6)$$

The total density of electrons in surface states at energies above the dark Fermi level is obtained by integration:

$$n_{\text{ss}} = \int_0^{qU_{\text{photo}}} f_{\text{ss}}(E) s_{\text{ss}}(E) dE \quad (7)$$

where $s_{\text{ss}}(E)$ is the density of states function for surface states and f_{ss} is the Fermi Dirac occupancy factor. Note that this expression assumes that the rate of electron exchange with the conduction band is faster than the rate of electron transfer to O, i.e., we are considering energies above the so-called demarcation level.²⁰ If electron traps are confined exclusively to the surface, n_{ss} represents the total trapped electron density.

Electron Transfer via the Substrate. In an electrode process, the rate of electron transfer to and from a conducting substrate generally is dependent on potential. If no blocking layers are present, the FTO behaves essentially as a noncatalytic metal, and in the absence of diffusion limitations,⁷ the total current density for a simple one electron-transfer redox reaction is given by the Butler Volmer equation,^{7,14,21} which can be written in terms of the photovoltage as

$$j_{\text{sub}} = j_0 \left[\exp\left(\frac{-(1-\alpha)nqU_{\text{photo}}}{k_{\text{B}}T}\right) - \exp\left(\frac{\alpha nqU_{\text{photo}}}{k_{\text{B}}T}\right) \right] \quad (8)$$

Here, j_0 is the exchange current density, α the cathodic transfer coefficient, and n the number of electrons transferred. Note that the photovoltage corresponds (with reversed sign) to the overpotential η that appears in the Butler Volmer equation for conventional electrode reactions, i.e., a positive photovoltage results in a negative (reduction) current at the FTO.

Therefore, the photostationary condition at open circuit is defined by

$$qI_{\text{abs}} = qI_0 \times \text{IPCE} = j_{\text{cb}} + j_{\text{ss}} + j_{\text{sub}} \quad (9)$$

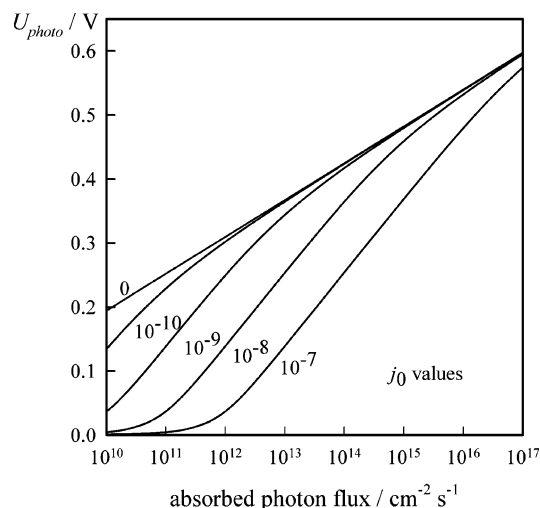


Figure 2. Intensity dependence of the photovoltage calculated for the case where electron transfer occurs only from the conduction band of the TiO_2 and from the conducting substrate; $k_{\text{cb}} = 10^6 \text{ s}^{-1}$, $k_{\text{ss}} = 0$, j_0 as shown. Other values used in the calculations include the following: TiO_2 film thickness, $10 \mu\text{m}$; $s_{\text{ss}}(0) = 5 \times 10^{15} \text{ cm}^{-3} \text{ eV}^{-1}$; $N_{\text{cb}} = 10^{21} \text{ cm}^{-3}$; $\beta = 0.25$; $\alpha n = 0.5$; and $E_{\text{cb}} - E_{\text{F,redox}} = 1.0 \text{ eV}$. Note that even small exchange current densities ($j_0 = 10^{-9} \text{ A cm}^{-2}$) lead to substantial deviations from ideality at low intensities. At sufficiently high intensities, back reaction via the conduction band dominates, giving ideal diode behavior.

where I_{abs} is the absorbed photon flux and I_0 is the incident photon flux (given in units of $\text{cm}^{-2} \text{ s}^{-1}$).

The relative importance of back reaction via the substrate is dependent on the thickness of the nanocrystalline film, because both j_{cb} and j_{ss} are dependent linearly on thickness, whereas j_{sub} is independent of thickness. It follows that back reaction via the substrate will be more important for thinner films of nanocrystalline TiO_2 .

Intensity Dependence of the Photovoltage. The intensity dependence of the photovoltage can be calculated from eq 9, because U_{photo} determines j_{cb} , j_{ss} , and j_{sub} . Model calculations were performed using an exponential distribution of surface states of the type found in previous studies.^{16,17} For convenience, we express the distribution in the simple form

$$s_{\text{ss}}(E) = s_{\text{ss}}(0) \exp\left[\frac{\beta(E - E_{\text{F,redox}})}{k_{\text{B}}T}\right] \quad (10)$$

where the energy zero is located at the redox Fermi level and $s_{\text{ss}}(0)$ corresponds to the density of states at $E = E_{\text{F,redox}}$. The β term describes the broadening of the exponential distribution. The current density at the substrate was calculated from eq 8, using different values of the exchange current density j_0 and $\alpha n = 0.5$.

Figure 2 illustrates the influence on the photovoltage of back reaction via the substrate for the case where back reaction via the surface states is negligible, i.e., electron transfer occurs only from the conduction band of the nanocrystalline TiO_2 and from the conducting substrate. In the absence of electron transfer via the substrate ($j_0 = 0$), the semilogarithmic plot of U_{photo} vs I_{abs} has a slope of 59 mV/decade, which is characteristic of an ideal diode (cf. eq 3). The other plots in Figure 2 show that even very low exchange current densities for the redox process at the substrate will cause significant deviations from ideality in the intensity dependence of the photovoltage, particularly at low light intensities. At high intensities, the plots tend toward ideal behavior; however, at lower intensity, the slope is determined

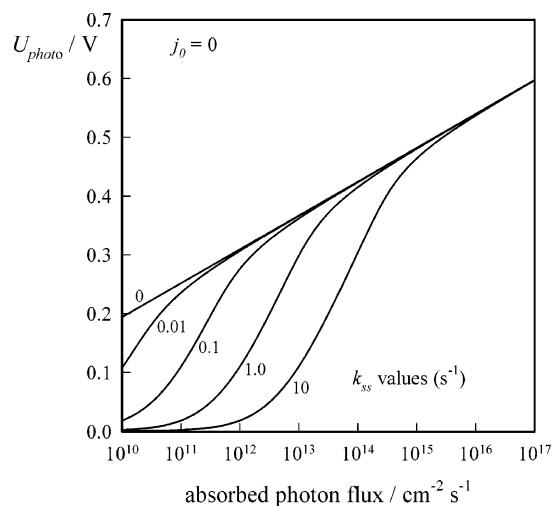


Figure 3. Calculated intensity dependence of the photovoltage for the case where electron transfer occurs only via the conduction band and surface states of the nanocrystalline TiO_2 . Note that the calculation assumes that all electron traps can exchange electrons with the redox species; $j_0 = 0$, $\beta = 0.25$, k_{ss} as shown, and other values are the same as those for Figure 2. Note the falloff in photovoltage due to reaction via surface states. At high intensities, back reaction via the conduction band dominates, giving ideal diode behavior.

by the Butler Volmer equation (eq 8), and for $\alpha n = 0.5$, the slope is 118 mV/decade. Because, in the absence of blocking layers, experimental values of j_0 for the I_3^-/I^- system range from 10^{-9} to $10^{-5} \text{ A cm}^{-2}$, depending on the type of conducting glass and the extent of cleaning, it is clear that a significant effect on the photovoltage behavior should be observed experimentally.

The influence of back reaction via the surface states is illustrated in Figure 3 for a situation in which electron transfer via the substrate is negligible (ideal blocking layer). For simplicity, it has been assumed that trap states are confined to the surface: the validity of this assumption is examined in the Results and Discussion section. Deviations from the ideal diode behavior are again evident at lower light intensities. This raises the central question of how one can distinguish experimentally between the two explanations for nonideal photovoltage behavior: reaction via the substrate or via the surface states. The only reliable way to distinguish between the two possibilities is to evaluate the influence of the blocking layer. This should affect only j_{sub} but not j_{ss} . It follows that, if using a blocking layer leads to near-ideal diode behavior, one can assume that back reaction via the substrate is more important than via the surface states in the absence of a blocking layer.

In the general case where back reaction occurs via all three routes, the relative contributions are intensity-dependent. These contributions were calculated from the fluxes calculated as a function of photovoltage and the photon/electron flux balance expressed by eq 9. Typical results are illustrated in Figure 4. Note that the conduction band route always dominates at high light intensities, whereas at lower intensities, the surface state and substrate routes become more important.

Experimental Section

Thin-layer cells were constructed by sealing FTO, heat-treated FTO, or spray-pyrolysis TiO_2 -coated FTO to sputter-coated platinum counter electrodes, using a $50 \mu\text{m}$ Surlyn gasket. The counter electrodes contained two holes, to allow filling of the redox electrolyte, which consisted either of 0.85 M methylhexylimidazolium iodide, 0.1 M LiI (anhydrous, 99.999% purity,

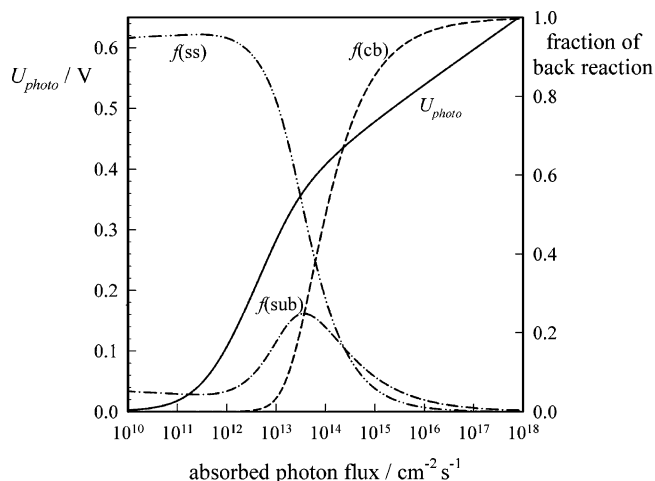


Figure 4. Photovoltage plot illustrating the case where all three back-reaction routes are operative; $j_0 = 10^{-9} \text{ A cm}^{-2}$, $k_{cb} = 10^6 \text{ s}^{-1}$, $k_{ss} = 1 \text{ s}^{-1}$, and $\beta = 0.25$. Other values are the same as those in Figure 2. Note that reaction via the conduction band dominates at high intensities, giving ideal diode behavior. At lower light intensities, reaction via surface states and via the substrate become more important, with surface states dominating at the lowest intensity.

Aldrich), 0.05 M I_2 (anhydrous, 99.999% purity, Aldrich), and 0.2 M *tert*-butylpyridine (99% purity, Aldrich) in acetonitrile or a mixture of 0.162 M $\text{Co(II)(dbbip)}_2^{2+}$ and 0.018 M $\text{Co(III)(dbbip)}_2^{3+}$ in 60% ethylene carbonate/40% acetonitrile.¹⁴ The filling holes were sealed with Surlyn and a glass cover slip. FTO plates were cleaned by sonication in 5% Deconex solution. They were then rinsed thoroughly and further cleaned by sonication in hot 2-propanol, followed by sonication in ethanol. Finally, they were dried in a stream of nitrogen before use. To investigate the effects of thermal treatment on electrochemical properties, some of the cleaned FTO plates were fired in a stream of air for 30 min at 450 °C before being used to make thin-layer cells. TiO_2 blocking layers²² were prepared as described previously,⁷ by spraying a 0.2 M solution of titanium di-isopropoxide bis(acetylacetonate) in 2-propanol onto the hot glass substrate (450 °C) in 25 short bursts over a period of 2 min. Different types of glass were used to make thin layer cells: Libby Owens Ford (LOF) TEC Glass (supplied by Hartford Glass, USA, 15 Ω), Asahi Glass (Asahi Glass, Japan, 12 Ω), and a different sample of LOF TEC glass (supplied by INAP Gelsenkirchen, 10 Ω).

Thin-layer cells with nanocrystalline TiO_2 films and dye-sensitized solar cells were prepared with different types of FTO glass, both with and without TiO_2 blocking underlayers. An aqueous nanocrystalline TiO_2 colloid was made by the acetic acid hydrolysis route, which is described elsewhere.^{4,5} The colloid was coated onto the prepared FTO via the doctor-blading technique, using two adhesive tape (Scotch Tape) spacers. The nanocrystalline films were fired in a stream of hot air at 450 °C for 30 min and placed overnight in a dye bath that consisted of 1.5 mM *cis*-bis(isothiocyanato) bis(2,2'-bipyridyl-4,4'-dicarboxylato)-ruthenium(II) bis-tetrabutylammonium (N719) in 50/50 acetonitrile/*tert*-butyl alcohol while still warm. The dyed films were removed, rinsed in acetonitrile, and dried in a stream of nitrogen before being sealed to a platinized counter electrode. Finally, the cells were filled with the same iodide redox electrolyte as that used for the thin-layer cells. The thickness of the nanocrystalline layers was determined by profilometry to be in the range of 5–10 μm . Similar results were obtained by firing the plates on a hot plate, instead of in a hot air stream.

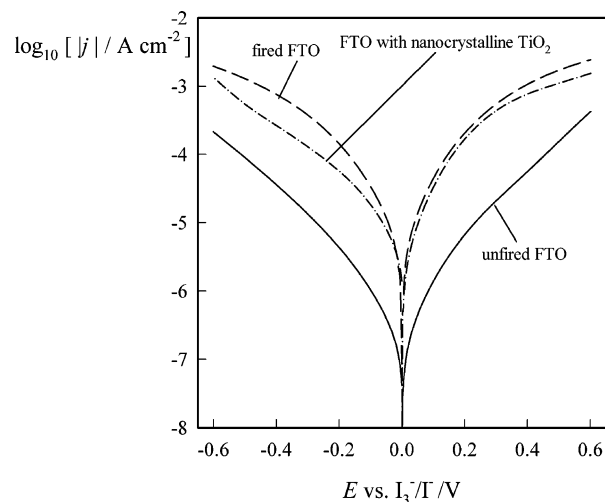


Figure 5. Tafel plots of current density versus cell voltage for thin-layer cells constructed with bare and nanocrystalline TiO_2 -coated LOF (Hartford) conducting glass. A tri-iodide/iodide electrolyte is used. Note that thermal treatment of the FTO increases the electron exchange rate by an order of magnitude; the enhanced exchange rate is also seen in the case of FTO coated with a sintered nanocrystalline TiO_2 layer.

Also, an oil-based colloidal preparation of nanocrystalline TiO_2 gave results that were similar to those of the aqueous colloid.

Tafel plots were measured using an Autolab PGSTAT 12 potentiostat (EcoChemie) operating in two-electrode mode. The scan rate was 10 mV/s. The dependence of the photovoltage on intensity was determined by illuminating the cells with a green diode laser ($\lambda = 532 \text{ nm}$). The intensity of the light was varied using Schott NG neutral density filters. Open-circuit voltage measurements were made using a high impedance low-noise preamplifier (Stanford Research Instruments).

Results and Discussion

Tafel Plots. Figure 5 illustrates the electrochemical behavior of three thin-layer cells that have been constructed using LOF (Hartford) conducting glass. The symmetrical Tafel plots for the uncoated electrodes indicate that the FTO electrode behaves essentially as a metal, so that the oxidation of I^- , as well as the reduction of I_3^- , is possible. What is striking here is that the heat treatment at 450 °C substantially enhances the electrochemical activity of the FTO. Details of the analysis of Tafel plots for this type of thin-layer cell have been given previously.⁷ In the present case, the analysis shows that the exchange current density for the I_3^-/I^- redox system at the LOF (Hartford) FTO electrode increases from $\sim 10^{-6} \text{ A cm}^{-2}$ to $10^{-5} \text{ A cm}^{-2}$ after heat treatment. Clearly, if a 10-fold enhancement of the back-reaction rate at the substrate occurs during processing of the nanocrystalline TiO_2 film at high temperature, it will degrade the cell performance under load conditions.

One might expect the activity of the FTO electrode to decrease when it is coated with a nanocrystalline layer of insulating TiO_2 . This would be evident in the right-hand branch of the Tafel plot, which should correspond only to oxidation of I^- at the FTO, because the redox energy of the I_3^-/I^- system is so far above the valence band of the TiO_2 that oxidation of I^- by hole injection can be ruled out. However, Figure 5 clearly shows that coating the FTO with the TiO_2 colloid and firing it at 450 °C has only a minor effect on the oxidation of I^- . This observation contrasts with the diode behavior observed when FTO electrodes are coated with a thin blocking layer of TiO_2 via spray pyrolysis. As we have shown previously, I^- oxidation is almost entirely suppressed in this case⁷ (also see Figure 8).

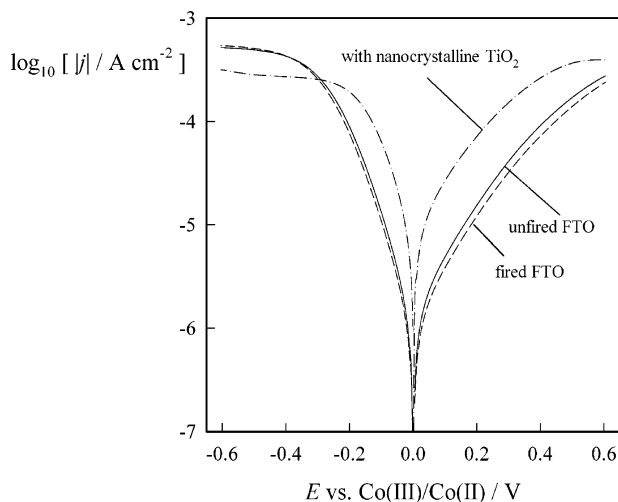


Figure 6. Tafel plots for cells constructed from LOF (Hartford) conducting glass. A Co(III)/Co(II) electrolyte is used. In this case, thermal treatment has little effect on the electron exchange rate, but coating with nanocrystalline TiO₂ enhances the rate markedly.

Therefore, it seems that the nanocrystalline TiO₂ layer does not block the FTO substrate in the way that might be expected on purely geometrical grounds.

The left-hand branch of the Tafel plot is the one that is relevant, as far as the operation of the DSC is concerned, because it corresponds to the reduction of I₃[−] by electrons. Comparison of the left-hand branches of the Tafel plot in Figure 5 for the unfired and heat-treated FTO clearly shows that the heat treatment enhances the activity of the FTO. In fact, the activity of the heat-treated FTO is higher than that of an electrode coated with nanocrystalline TiO₂ and fired for the same time. This suggests that, for the latter type of electrode, the dominant route involves electron transfer from the FTO driven by the overvoltage (or, in the case of a DSC, by the photovoltage), rather than electron transfer from the bulk of the nanocrystalline TiO₂ film. The current density of the nanocrystalline TiO₂ electrode at −0.6 V (corresponding to a photovoltage of 0.6 V) can be estimated from Figure 5 to exceed 1 mA cm^{−2}. This would correspond to a loss of >10% of the total power efficiency for a DSC operating at the maximum power point at 1 sun with a current density of 10 mA cm^{−2}.

Because it is known that the I₃[−]/I[−] redox system can be catalyzed by dissociative adsorption of I₂ on metals such as platinum, it is likely to be sensitive to trace impurities that can act as catalytic sites on the FTO. To check whether the observed enhancement in activity of the FTO after heat treatment was due to an increase in surface roughness or due to a specific catalytic effect, cells were fabricated using the Co(III)(dbbp)₂^{3+/2+} redox electrolyte, which behaves as an outer sphere redox system, where catalysis is not expected. Figure 6 illustrates the Tafel plots obtained in this case for cells without and with thermal treatment, as well as for a cell with a film of nanocrystalline TiO₂. The currents are higher than with the I₃[−]/I[−] redox system, reflecting a higher value of *j*₀. In addition, diffusion-controlled limiting currents are observed at high voltages, as a consequence of the slow diffusion of the cobalt complex in the rather-viscous solvent mixture.¹⁴ It is clear that, in this case, thermal treatment has little effect on the rate of the electrode process, which shows that the enhancement effect observed in the case of I₃[−]/I[−] is due to catalysis of some type, possibly because of the presence of impurities introduced by the heat treatment. More surprising is the observation that the presence of the nanocrystalline TiO₂ layer enhances the current

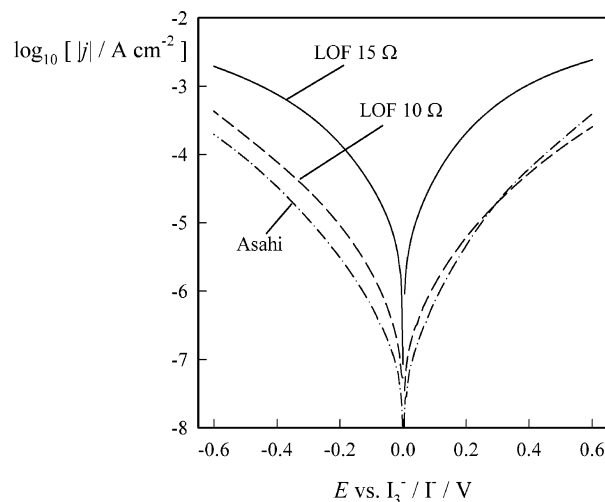


Figure 7. Comparison of the current voltage behavior of thin layer cells constructed with different types of FTO-coated conducting glass (heat treated; a tri-iodide/iodide electrolyte is used).

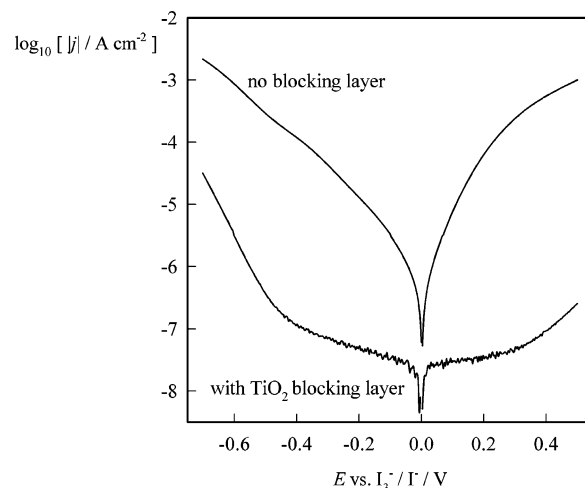


Figure 8. Tafel plots for LOF glass (Hartford, 15 Ω), showing the effect of a thin TiO₂ blocking layer. Tri-iodide/iodide electrolyte is used.

in both branches of the Tafel plot for the cobalt redox system. The enhancement of the right-hand branch of the Tafel plot suggests that a thin layer of TiO₂ near the FTO may be active in the oxidation of the Co(II) complex. For this to occur, some type of tunneling process is necessary, and one possibility is that the heat-treatment results in the formation of a highly doped thin layer of TiO₂ near the FTO interface. The effect is not observed when a TiO₂ blocking layer is used.

The activity of the FTO for electron exchange with the I₃[−]/I[−] redox system varies not only with sample preparation, but also according to the glass supplier. Figure 7 contrasts the Tafel behavior of three different sample types. It can be seen that the activity of the FTO-coated glass varies considerably from sample to sample, with the LOF (Hartford) glass having the highest exchange current density. The observed variations in *j*₀, by more than an order of magnitude, indicate that unpredictable and largely uncontrollable losses will occur in cells without blocking layers.

The influence of a TiO₂ blocking layer on the electrochemical behavior of the I₃[−]/I[−] redox system is illustrated in Figure 8. The layer suppresses the oxidation of I[−] almost completely, as well as the reduction of I₃[−] at voltages less negative than −0.5 V. The steep rise in current observed at more-negative potentials is due to electron accumulation in the nanocrystalline film under

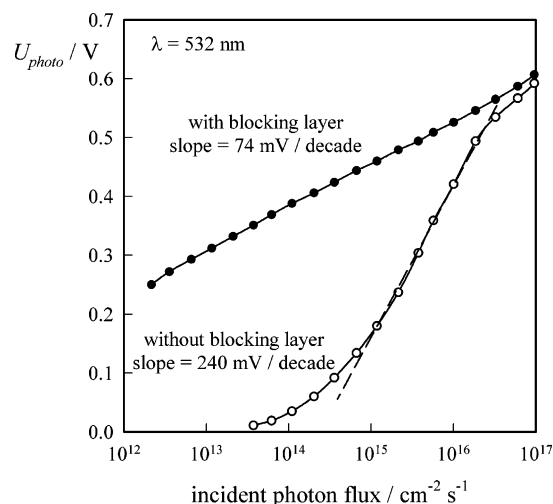


Figure 9. Intensity dependence of the photovoltage for DSCs constructed from Asahi conducting glass with and without TiO_2 blocking layers. Note, in particular, the linear response down to very low light intensities that is observed when a blocking layer is used. The experimental data can be compared with the calculated results in Figure 2.

conditions where the blocking layer is no longer fully depleted.⁷ The electrochemical results suggest that much more ideal behavior should be observed if a blocking layer is used in DSCs based on the I_3^-/I^- redox system as well as on the cobalt complex.

Photovoltage as a Function of Illumination Intensity. The intensity dependence of the photovoltage in DSCs has been reported by several groups. Liu et al.²³ reported an average slope of 64 mV/decade for measurements using white light in the range of 0.1–100 mW cm^{-2} . Huang et al.²⁴ obtained similar values using the same intensity range. Our more recent work,⁶ which used monochromatic illumination over a wider intensity range (10^{11} – 10^{16} $\text{cm}^{-2} \text{ s}^{-1}$), gave a slope of 85 mV/decade at high intensities but showed a falloff in the plot below 10^{14} $\text{cm}^{-2} \text{ s}^{-1}$, which was attributed to shunting of the cell by back reaction at the substrate. This falloff would not have been visible in the studies by Liu et al.²³ and Huang et al.,²⁴ because the intensity range that they used corresponds approximately to a monochromatic photon flux density of 10^{14} – 10^{17} cm^{-2} .

The analysis given in the theoretical section shows that DSCs without blocking layers should give nonideal plots of photovoltage as a function of light intensity, particularly at low light intensities. On the other hand, in the ideal case, where no back reaction occurs at the substrate or via the surface states, the slope of the semilogarithmic plot of U_{photo} versus the photon flux should be 59 mV/decade at 298 K over the entire intensity range. The experimental result shown in Figure 9 for a cell with a blocking layer shows almost-ideal linear behavior over a wide intensity range, down to very low photon fluxes that correspond to current densities of $<10^{-8}$ A cm^{-2} . By contrast, the DSC without a blocking layer gives a much less ideal plot that corresponds closely to the predictions of the model in the case where back reaction via the substrate is important.

The effect of the blocking layer on the intensity dependence of the photovoltage is reproducible, and all DSCs constructed using blocking layers exhibited linear semilogarithmic plots with slopes in the range of 60–75 mV/decade, regardless of the type of FTO glass used. By contrast, a much wider variation in behavior was observed for DSCs without blocking layers. This is expected, because the study has shown that the activity of the FTO toward the back reaction is dependent on a range of

factors, such as the type of glass and the thermal treatment. A further factor that must be considered is the cleaning of the glass. Different protocols are likely to give different values of j_0 , so that “good” cells may, in fact, be cells in which contamination of the FTO reduces the value of j_0 .

The observation that linear photovoltage plots with almost-ideal slopes can be obtained if blocking layers are used provides strong evidence that back reaction via the substrate rather than via the surface states is responsible for nonideal photovoltage behavior. The remaining small deviations from ideality, in the case of films with blocking layers, may suggest a small contribution from the surface states, although other effects, such as band edge unpinning, may be responsible.

The comparison of experimental and theoretical photovoltage plots raises an interesting point. The global rate constant for reaction via surface states clearly must be many orders of magnitude smaller than the rate constant for reaction via the conduction band to explain the observed results if one makes the assumption that the majority of electron trap states are located at the surface of the nanocrystallites. As Figure 3 shows, k_{ss} must be $<0.01 \text{ s}^{-1}$ to give a linear plot down to $10^{11} \text{ cm}^{-2} \text{ s}^{-1}$. This contrasts with the rate constant of 10^6 s^{-1} used for k_{cb} in the calculations. A difference of 8 orders of magnitude in rate constants cannot be explained on energetic grounds, and we therefore conclude that the great majority of the states involved in electron trapping are, in fact, located in the bulk of the TiO_2 nanocrystals precluding electron exchange with redox species. If this is the case, then electrons can only reach the surface by thermal release into the conduction band, followed by transport to the surface. Because $\sim 5\%$ of the atoms in the nanocrystal are in the surface, we conclude that the interaction of surface atoms with the dye and with components of the electrolyte may reduce the electron trap density, relative to the bulk.

Conclusions

The importance of the back reaction of electrons via the substrate has been unjustifiably neglected in the majority of published work, including our own. The results of the present study show that, although this process may be negligible under certain conditions (short circuit, high light intensities), it becomes more important under open-circuit conditions and at low light intensities. Consequently, mechanistic inferences derived from studies of the intensity dependence of parameters, such as the electron lifetime in DSCs without blocking layers, may need to be re-examined. The implications for the interpretation of dynamic measurements are considered elsewhere.¹⁵

Acknowledgment. P.J.C. thanks the University of Bath and Johnson Matthey for support. The authors thank Prof. S. Yanagida (Osaka University) for the donation of the Asahi glass samples, INAP Gelsenkirchen for the donation of the Libby Owens Ford (LOF) glass, Dr. R. J. Potter (Johnson Matthey) for the donation of the Hartford LOF glass, Dr. S. M. Zakeeruddin (École Polytechnique Fédérale de Lausanne (EPFL)) for donation of the cobalt complex, and Dr. A. B. Walker (University of Bath) for useful discussions. S.H. acknowledges financial contribution from the European Union (contract number NNE5-2001-00192) Nanomax.

References and Notes

- (1) O'Regan, B.; Grätzel, M. *Nature* **1991**, *353*, 737.
- (2) Nazeeruddin, M. K.; Splanillo, R.; Liska, P.; Comte, P.; Grätzel, M. *Chem. Commun.* **2003**, 1456.

- (3) Lindstrom, H.; Rensmo, H.; Sodergren, S.; Solbrand, A.; Lindquist, S. E. *J. Phys. Chem.* **1996**, *100*, 3084.
- (4) Peter, L. M.; Wijayantha, K. G. U. *Electrochem. Commun.* **1999**, *1*, 576.
- (5) Peter, L. M.; Wijayantha, K. G. U. *Electrochim. Acta* **2000**, *45*, 4543.
- (6) Fisher, A. C.; Peter, L. M.; Ponomarev, E. A.; Walker, A. B.; Wijayantha, K. G. U. *J. Phys. Chem. B* **2000**, *104*, 949.
- (7) Cameron, P. J.; Peter, L. M. *J. Phys. Chem. B* **2003**, *107*, 14394.
- (8) Nusbaumer, H.; Moser, J. E.; Zakeeruddin, S. M.; Nazeeruddin, M. K.; Grätzel, M. *J. Phys. Chem. B* **2001**, *105*, 10461.
- (9) Sapp, S. A.; Elliott, C. M.; Contado, C.; Caramori, S.; Bignozzi, C. A. *J. Am. Chem. Soc.* **2002**, *124*, 11215.
- (10) Nusbaumer, H.; Zakeeruddin, S. M.; Moser, J. E.; Grätzel, M. *Chem.—Eur. J.* **2003**, *9*, 3756.
- (11) Bach, U.; Krueger, J.; Grätzel, M. *Proc. SPIE—Int. Soc. Opt. Eng.* **2001**, *4108*, 1.
- (12) Krüger, J.; Plass, R.; Cevey, L.; Piccirelli, M.; Grätzel, M.; Bach, U. *Appl. Phys. Lett.* **2001**, *79*, 2085.
- (13) Krüger, J.; Plass, R.; Grätzel, M.; Cameron, P. J.; Peter, L. M. *J. Phys. Chem. B* **2003**, *107*, 7536.
- (14) Cameron, P. J.; Peter, L. M.; Zakeeruddin, S. M.; Grätzel, M. *Coord. Chem. Rev.* **2004**, *248*, 1447–1453.
- (15) Cameron, P. J.; Peter, L. M. Manuscript in preparation, 2004.
- (16) Duffy, N. W.; Peter, L. M.; Rajapakse, R. M. G.; Wijayantha, K. G. U. *Electrochem. Commun.* **2000**, *2*, 658.
- (17) Peter, L. M.; Duffy, N. W.; Wang, R. L.; Wijayantha, K. G. U. *J. Electroanal. Chem.* **2002**, *524*, 127.
- (18) Schlichthörl, G.; Huang, S. Y.; Sprague, J.; Frank, A. J. *J. Phys. Chem. B* **1997**, *101*, 8139.
- (19) Schlichthörl, G.; Park, N. G.; Frank, A. J. *J. Phys. Chem. B* **1999**, *103*, 782.
- (20) Bisquert, J.; Zaban, A.; Salvador, P. *J. Phys. Chem. B* **2002**, *106*, 8774.
- (21) Bard, A. J.; Faulkner, L. R. *Electrochemical Methods: Fundamentals and Applications*, 2nd ed.; Wiley: New York, 2001.
- (22) Kavan, L.; Grätzel, M. *Electrochim. Acta* **1995**, *40*, 643.
- (23) Liu, Y.; Hagfeldt, A.; Xiao, X. R.; Lindquist, S. E. *Sol. Energy Mater. Sol. Cells* **1998**, *55*, 267.
- (24) Huang, S. Y.; Schlichthörl, G.; Nozik, A. J.; Grätzel, M.; Frank, A. J. *J. Phys. Chem. B* **1997**, *101*, 2576.